

Characterization of an LED Based Photoreactor to Degrade 4-Chlorophenol in an Aqueous Medium Using Coumarin (C-343) Sensitized TiO₂

Jyoti P. Ghosh,[†] Cooper H. Langford,^{*,‡} and Gopal Achari^{*,†}

Department of Civil Engineering and Department of Chemistry, University of Calgary, 2500 University Drive NW, Calgary, Alberta, Canada T2N 1N4

Received: May 16, 2008; Revised Manuscript Received: July 23, 2008

A detailed performance evaluation of a simple high intensity LED based photoreactor exploiting a narrow wavelength range of the LED to match the spectrum of a dye in a photocatalysis system is reported. A dye sensitized (coumarin-343, $\lambda_{\text{max}} = 446$ nm) TiO₂ photocatalyst was used for the degradation of 4-chlorophenol (4-CP) in an aqueous medium using the 436 nm LED based photoreactor. The LED reactor performed competitively with a conventional multilamp reactor and sunlight in the degradation of 4-CP. Light intensities entering the reaction vessel were measured by conventional ferrioxalate actinometry. The results can be fitted by approximate first order kinetic behavior in this system. Hydroxyl radicals were detected by spin trapping EPR, and effects of OH radical quenchers on kinetics suggest that the reaction is initiated by these radicals or their equivalents. LEDs operating at competitive intensities offer a number of advantages to the photochemist or the environmental engineer via long life, efficient current to light conversion, narrow bandwidth, forward directed output, and direct current power for remote operation. Matching light source spectrum to chromophore is a key.

Introduction

The rapid recent progress on high output inexpensive light emitting diodes (LEDs) opens questions for design of LED based photoreactors which have, among other advantages, the capacity to be chosen tuned to chromophore absorption bands. The LEDs offer the photochemist several advantages. These include a new source of “tunable” approximately monochromatic light, long lifetime, and efficient electricity to light conversion (little heating). In engineering practice, DC power offers greater flexibility for field application.

The degradation of organic pollutants in aqueous systems exploiting TiO₂ photocatalysis is well-known.¹ Although TiO₂ is the most extensively used photocatalyst, its high band gap energy of about 3.2 eV seriously limits its ability to adsorb light with wavelengths >385 nm. Much effort has been expended on extending photocatalyst absorbance into the visible, and dye sensitization has been one major direction.^{2–6} Success with dye sensitization opens options for use of sunlight. However, high reaction rates require intense light in the appropriate spectral region. Dyes are best used with sources well-matched to their absorption spectra, which can be achieved with a choice of a high intensity LED.

In dye sensitized photocatalysis, a dye absorbing visible light excites an electron from the HOMO (highest occupied molecular orbital) of a dye to the LUMO (lowest unoccupied molecular orbital). The excited electron can be injected from the excited-state dye to TiO₂ conduction band provided the reduction potential of the excited state is found to be more negative than the conduction band of TiO₂. As a result, the dye is converted to a cationic radical, and the injected electron in the TiO₂

conduction band can reduce the surface-sorbed oxygen producing $\cdot\text{O}_2^-$ or $\cdot\text{OOH}$ as a reactive species that can also disproportionate to give $\cdot\text{OH}$.^{4–9} Degradation of organic dyes using TiO₂ and visible light has been widely reported.^{5,6,10–13} TiO₂ particles sensitized by, for example, $-\text{COOH}$ substituted ruthenium bipyridyl complexes are reactive¹³ and Cho et al.¹⁴ reported decomposition of CCl₄ by visible light irradiation of TiO₂ particles with attached Ru(bipy)₃²⁺ complexes.

A number of studies have exploited LED light sources for photocatalysis,^{15–17} but to our knowledge there has been only one report so far evaluating any special characteristics of an LED-based photoreactor, and it did not provide detailed information on intensity utilization or comparison to competitive light sources.¹⁷ The main motivation for this paper is to evaluate the competitiveness of LED sources versus conventional Hg lamp based and sunlight options. (Neither of our laboratory reactors are engineering optimized, but the LEDs are driven by ~12 W of power and the Hg lamps are driven by ~112 W.) Coumarin (C343; $\lambda_{\text{max}} = 446$ nm) adsorbed on TiO₂ was chosen as a test case with a 436 nm LED array using the model pollutant chlorophenol as an oxidizable substrate. Coumarin dyes on TiO₂ have been reported in photovoltaic systems^{18–21} and reported to yield efficient solar cells with nanocrystalline TiO₂.²² Halogenated organics, both aliphatic and aromatic, have been widely investigated target compounds for photocatalytic degradation, and 4-chlorophenol (4CP) has become a standard for the evaluation of reaction parameters.^{23–27}

Hence the objective of this work is to characterize a blue LED based reactor for the degradation of 4-CP using coumarin-343 coated TiO₂. The reaction pathway which displays some novelty is also investigated.

Experimental Section

Materials. 4-Chlorophenol (+99%), 4-chlorocatechol (97%), catechol (99%), 1,10-phenanthroline, 1,2,4-benzenetriol, cou-

* Corresponding author. Telephone: (403) 220 3228. E-mail: chlangfo@ucalgary.ca (C.H.L.). Telephone: (403) 220 6599. Fax: (403) 282 7026. E-mail: gachari@ucalgary.ca (G.A.).

[†] Department of Civil Engineering.

[‡] Department of Chemistry.

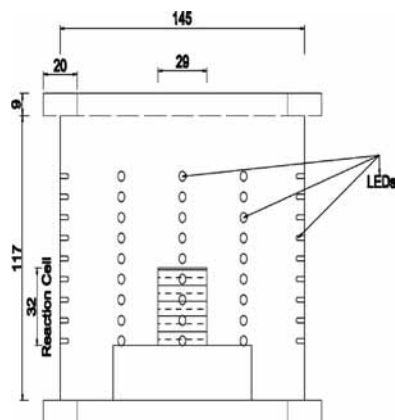


Figure 1. Longitudinal cross-section of the LED reactor. (All dimensions are in millimeters.)

marin dye (C-343), 5,5-dimethyl-1-pyrroline *N*-oxide (DMPO, 97%), 2,2,6,6-tetramethyl-4-piperidone (4-oxo-TMP, 95%), ethyl alcohol, and ortho-phosphoric acid (85–90%, for HPLC) were purchased from Sigma Aldrich. HPLC grade acetonitrile (99.8%), dimethylsulfoxide (DMSO), and sulfuric acid were purchased from EMD Chemicals Inc. (Missisaga Ontario). Nitric acid (68–70%) and sodium acetate (99–100.5%) were supplied by BDH Inc. Dihydroxymaleic acid was obtained from City Chemicals. Ferrous ammonium sulfate, sodium acetate, potassium chromate, and sodium azide (+99%) were obtained from Fischer Scientific Company. Potassium tris-oxaloferrate (m) the actinometer was synthesized in laboratory following established methods.²⁶ P25 TiO₂ was provided by Degussa Corporation. Distilled deionized water was used for all of the experiments.

Photocatalyst Preparation. A 3.00×10^{-4} M stock solution of C-343 dye was prepared by dissolving in a suitable amount in ethanol. An aqueous suspension containing 15 g/L of TiO₂ was separately prepared. A 5 mL sample of dye solution was then gently added to a 20 mL aqueous suspension of TiO₂ in an acidic environment. The slurry was manually stirred and allowed to stand for an hour. The solid was then separated by centrifugation for 20 min, and the supernatant was decanted. The dye coated TiO₂ was taken from the centrifuge tube, vacuum filtered, and oven-dried at 105 °C for 12 h. The dried photocatalysts were powdered and homogenized by mortar and pestle and stored for use.

Photocatalysts with different dye doping were prepared following the same procedure, adjusted stoichiometrically. Loading of the dye on TiO₂ was estimated from spectrophotometric measurement described as follows: The concentration of dye in the original dye solution in ethanol as diluted and the residual concentration of dye after the adsorption by TiO₂ particles in the aqueous solution was measured. The dye adsorbed was calculated from the difference. In practice, essentially 100% of the dye was adsorbed. The dye exhibited no significant water solubility.

Characterization of the Test LED Reactor. The LED reactor depicted in Figure 1 was constructed according to the authors' specifications. Electronic design and fabrication was done by HF Research, Medicine Hat, Alberta. Internal diameter of the reactor is 12.5 cm, and height is 13.5 cm. It is equipped with 81 Gilway "super bright" (Peabody, MA) E472 60 μ W (max. output) LEDs (The cost is \$1.10 per lamp, totalling \$89.10. Compare 14, 8 W Rayonnet fluorescents at \$140.) "Mega-bright" units are available with an order of magnitude higher output). Output is centred at 436 nm. The LED cylinder is mounted on a stirring plate and a covered glass reaction vessel

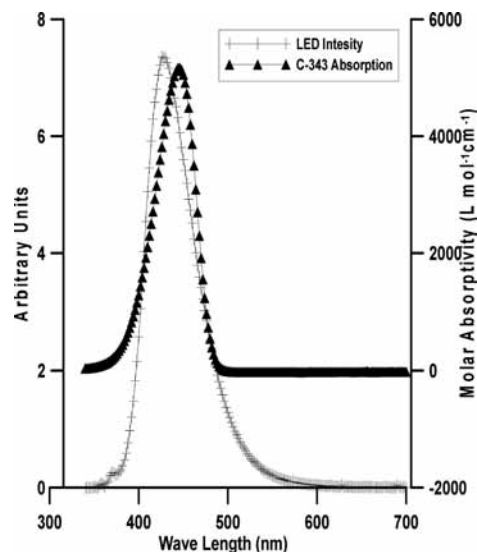


Figure 2. Molar absorptivity of coumarin-343 and intensity of LED's as a function of wavelength. LED intensity is given in arbitrary units on the left since measurements made on the single LED depend on distance from the sensor.

may be placed concentrically in the bottom of the light well. The maximum intensity of LEDs used in the reactor was confirmed at 436 nm by HF Research. Figure 2 gives the relative intensity of the LED's as a function of wavelength, overlaid by the absorption spectrum of C-343.

Light intensities entering the reaction vessel used were measured by conventional ferrioxalate actinometry.²⁸ The intensity of the light entering the vessel, placed in the LED reactor, was found to be 0.10 mW cm^{-2} . This can be compared to intensity in the conventional Rayonnet reactor equipped with 14, 8 W visible range fluorescent tubes, estimated by actinometry as 0.14 mW cm^{-2} in the 400–480 nm regions. Sunlight at one sun is estimated to give 0.06 mW cm^{-2} in the 380–480 nm range.

4-CP Assay. Concentrations of 4-CP and reaction intermediates were monitored by high performance liquid chromatography (HPLC, Model "Waters 486"). A reverse phase C₁₈ column (Phenomenex Gemini™ 5 μ , 250 \times 4.60 mm) was used for the separation with 10 μ L injections. Isocratic elution with a solvent mixture of 50% acetonitrile and 50% deionized water was applied at a flow rate of 1 mL min^{-1} . The wavelength used in the UV detector was 290 nm. Good separation of compounds was observed within a run of 10 min. The quantification of CP was accomplished by using the "Millennium Chromatography Manager" software. Concentration peak area relations were established from a linear calibration curve.

Intermediate Identification. The intermediates formed during the photocatalytic degradation of 4-CP were identified by comparison to retention time of knowns and by mass spectrometry with electrospray ionization. Irradiated samples from the reaction vessel were filtered with Filtropur syringe filters (0.2 μ m) and injected directly to the mass spectrometer (Bruker Esquire 3000) via an infusion pump (Cole Parmer 74900 series) at a rate of $4 \mu\text{L min}^{-1}$. Electrospray ionization was carried out in both positive and negative polarity modes. The drying gas was from liquid nitrogen, and the nebulizer was 7.0 psi. The pressure in the analyzer region was about 1.2×10^{-5} mbar. Data were acquired using Esquire Control Version 5.0 software.

Absorption Spectrum of Dye and Substrate. The UV–vis absorption spectra of dye solution in ethanol and substrate in aqueous solution were recorded with the corresponding solvent

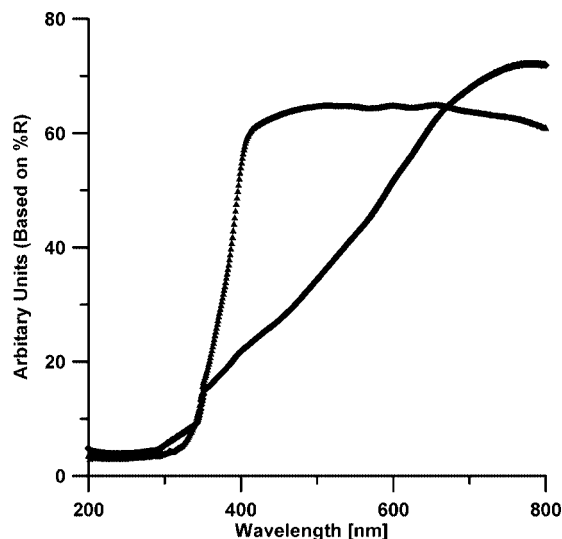


Figure 3. Reflectance spectrum of TiO₂ (P-25) is the upper curve reaching level reflectance from ~400 nm, and dye coated TiO₂ is the lower curve with reflectance changing in the 400 to 600 nm region.

as blank at room temperature on a Hewlett-Packard 8452 diode array spectrophotometer equipped with a computer for data acquisition. A quartz cell of 1 cm optical path length was used for all measurements. Reflectance spectra (shown in Figure 3) of TiO₂ and the dye loaded solid were recorded on the Cary 5000 UV-vis spectrophotometer (Varian), using the diffuse reflectance accessory. Before the UV analysis, the xerogels were finely ground, dispersed with methanol, and coated on glass substrate followed by drying at 80 °C for 8 h.

Detection of Reactive Oxygen Species. Spin trapping experiments^{29,30} to detect hydroxyl radicals were conducted by irradiation of the slurry containing the C-343/TiO₂ (1 g 100 mL⁻¹) in an aqueous solution of CP (initial concentration 100 ppm) in presence of DMPO. The DMPO concentration was kept at 5 mM in the solution.³¹ Aliquots of 1 mL were withdrawn from reaction vessel at proper intervals and filtered by using Filtrapor syringe filters (0.2 μm). The filtered samples were subsequently analyzed by electron spin resonance (ESR) for the presence of the DMPO-•OH adduct. The ESR spectra were recorded at room temperature using a Bruker EMX 10/12 Spectrometer equipped with a 12 kW power supply operating at X band frequencies. During the analysis, the instrument conditions were as follows: center of magnetic field, 3490 G; scan range, 120 G; modulation amplitude, 4 G; receiver gain, 1.78 × 10⁵; microwave frequency, 9.773 GHz; microwave power, 12.69 mW; time constant 40.76 ms; scan time, 20.972 s; number of scans 100. Data acquisitions and instrument control was achieved by WinEPR Acquisition, version 4.32 software. To confirm a role for hydroxyl radical in the reaction, tert-butyl alcohol scavenging was carried out at a pH of 6.2. The reaction mixtures were prepared to produce a tertiary-butyl alcohol concentration of 0.1 M.³² Azide quenching³³ experiments (azide concentration 0.1 M) were carried out at a pH of 10.8 as test for the role of singlet oxygen in the reaction.

Photochemical Protocol. Experiments on photocatalytic activity of the dye (C-343) coated TiO₂ were conducted in duplicate in the 2.9 cm diameter, 3.2 cm high cylindrical glass vial in an aqueous medium. The initial solution volume was 20 mL. The vessel was placed at the center of the LED reactor and irradiated.

Control experiments in the absence of photocatalyst, with Degussa P25, and in dark were conducted separately to confirm

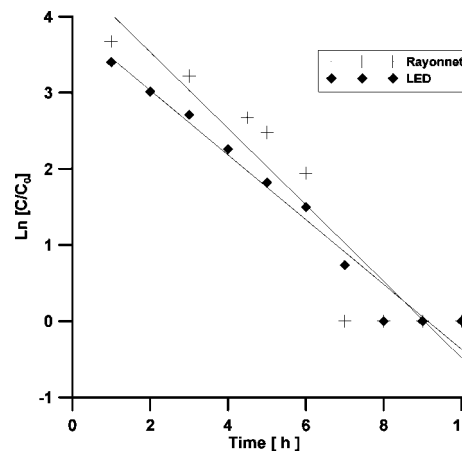


Figure 4. Logarithmic first order fit of the disappearance of 4-CP as a function of time in the presence of dye coated TiO₂. Substrate concentration is 40 ppm; catalyst loading is 3 g per 100 mL⁻¹. (+) Rayonnet, (♦) LED.

that no reaction is taking place in the absence of photocatalyst and light and to estimate the (small) dark adsorption of substrate by the photocatalyst. Photocatalytic experiments in a conventional Rayonnet reactor were conducted with the 2 cm diameter, 30 mL cylindrical reaction cell placed at the center of a cylindrical glass cell (8 cm dia, 450 mL). A potassium chromate solution (1 mM K₂CrO₄ in 0.22 M Na₂CO₃ aqueous solution) was introduced in between the glass vial and the outer glass wall as a filter limiting irradiation to visible light ($\lambda > 400$ nm). The reaction solutions were the same as those used in the LED.

Runs were conducted at various levels of loading of photocatalyst and for a series of dye levels on the photocatalyst. Reaction mixtures were equilibrated in dark for 15 min before the irradiation. The reactors remained open and were stirred during the reaction by using Teflon-coated stir bars. All of the experiments were conducted at room temperature (22 °C). At proper time intervals, 1 mL aliquots were withdrawn and filtered through 0.2 μm membrane filters. The short-term stability of the dye was estimated by repeat runs on a catalyst sample used in determination of the rate constant. There was a 15% decrease.

Results

Reaction Kinetics. The reaction of 4-CP under visible light irradiation in the LED based reactor used an initial concentration of 40 ppm and 1.0 to 4.0 g per 100 mL⁻¹ of reaction slurry. The disappearance of 4-CP as a function of time at 0.10 mW cm⁻² intensity was monitored. The reaction kinetics fitted approximately to first order and approached a limiting value at a loading of 3.0 g 100 mL⁻¹ of photocatalyst. Comparison runs were carried out in the conventional Rayonnet reactor equipped with 14, 8 W visible lamps (intensity 0.14 mW cm⁻²). Figure 4 shows the first order kinetics of 4-CP loss in both reactors at a loading of 3 g, 100 mL⁻¹. Rate constants fitted are $k_{LED} = 1.30 \times 10^{-4} \text{ s}^{-1}$ and $k_{Rayonnet} = 1.48 \times 10^{-4} \text{ s}^{-1}$. (These intensities and the band overlap with the dye are sufficiently close that reaction pathway is lamp independent.) Studies on kinetics of 4-CP loss were conducted with both higher and lower dye levels than that for Figure 4. The dye levels were varied in a range of 0.25×10^{-8} to $2.0 \times 10^{-8} \text{ mM g}^{-1}$. A three-dimensional diagram (Figure 5) shows rate as a function of dye level and photocatalyst loading. The peaks of the “pyramids” are the experimental points.

Reactive Oxygen Species and Reaction Intermediates. Candidate reactive oxygen species, generated in dye photocatalysis, are superoxide radicals (O₂•⁻), their disproportionation

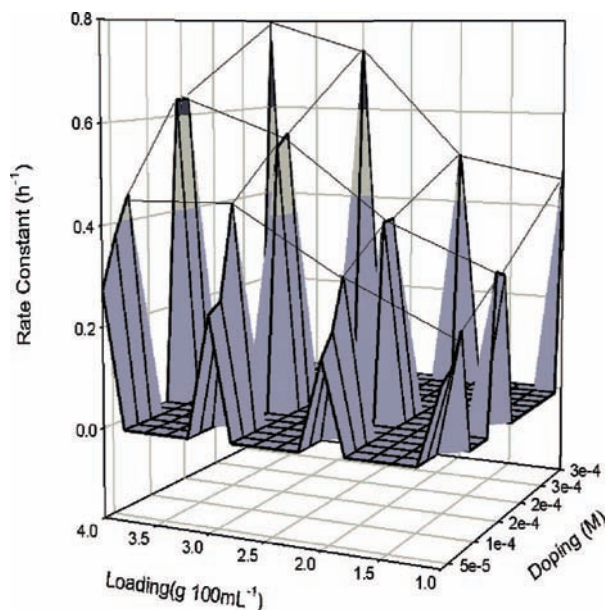


Figure 5. Three dimensional representations of apparent rate constants as affected by different dye doping concentration and catalyst loading. The experimental points are the tops of the pyramids.

product hydroxyl radicals ($\text{OH}\cdot$), and singlet oxygen ($^1\text{O}_2$).^{11,26} EPR spectra (not shown), obtained after various periods of irradiation, gave the signature 4-line signal of the DMPO adduct of the $\text{OH}\cdot$ radical. Unfortunately, this does not provide unambiguous evidence for an ROS involved here since the O_2 -adduct of DMPO can react thermally to give the $\text{OH}\cdot$ radical adduct. In order to evaluate the kinetic role of $\text{OH}\cdot$, scavenging experiments were carried out with *tert*-butanol (tOH scavenger) and azide ($^1\text{O}_2$ scavenger). Whereas butanol led to nearly 100% suppression of reaction, NaN_3 at 0.1 M concentration led to only modest rate reduction. This leads to the suggestion that reaction is initiated by the $\text{OH}\cdot$ radical, but other ROS may participate in the overall mechanism of degradation. Such complexity is indicated by a somewhat different pattern of intermediates than is typical for TiO_2 photocatalyzed oxidation of phenolic compounds.³⁴

Several intermediates, during the degradation of 4-CP have been identified by comparison of HPLC retention times to authentic samples and with molecular mass identified by electrospray ionization mass spectrometry. The major species identified as reaction intermediates were 1,2,4-benzenetriol and dihydroxymaleic acid. We were initially unable to find any chlorocatechol or any chlorine containing compounds that would be readily recognized in mass spectrometry by the isotopic satellite peak, but these may be formed and be consumed faster than they are formed.

The formation of dihydroxymaleic acid indicates successful ring cleavage. The important role of 1,2,4-benzenetriol underlines successful dechlorination, an important step in halocarbon degradation. Loss of 4-CP with formation of 1,2,4-benzenetriol and dihydroxymaleic acid as a function of time is shown in Figure 6.

Discussion

The central purpose of this study was evaluation of the prospects for use of LEDs as light sources competitive with currently widespread options. It is clear that the photochemist can benefit from the narrow spectral region output of LEDs to study processes at particular wavelengths since the LED

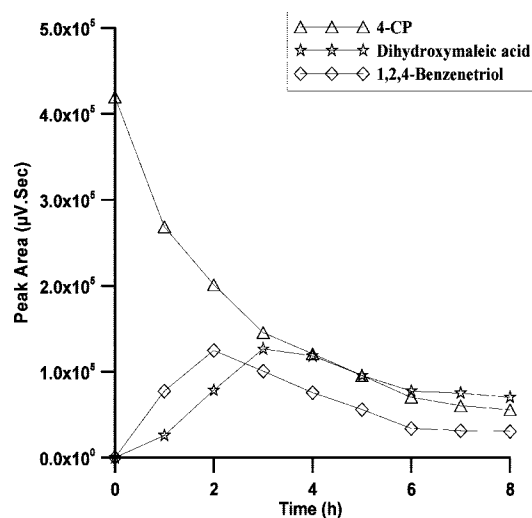


Figure 6. Degradation of 4-CP (Δ) and formation of 1,2,4-benzenetriol (\diamond) and dihydroxymaleic acid (\star), each as a function of time measured by HPLC peak areas.

becomes most competitive when matched to the spectrum of the chromophore. With the rapid progress of LED technology, intense LED systems from the UV to the red should be available now or very soon. In practical terms, LEDs offer high electrical to light energy conversion with little heat production, forward directed output facilitating delivery to a target, long lifetime, and operation on DC which may facilitate use in remote locations such as field instruments and pollution abatement activity.

The apparent rate constants in the LED and Rayonet reactors at the same photocatalyst loading show only a small difference, less than the calculated intensity difference across the coumarin band. The output of the fluorescent tubes rises monotonically across the 400 to 480 nm band³⁸ where coumarin absorbance is falling in the longer wavelength region. Thus, the coumarin dye harvests a larger fraction of energy from the well-matched LED unless absorbance at all wavelengths is large enough to harvest 100% of the incident light. The long wavelength part of the 380–480 region is not as effective with the fluorescent lamps as with the LEDs. The same point would apply to a run in sunlight. The explanation is confirmed by the effect of loading on apparent rate constants. The result indicates that the fluorescent lamp system with higher intensity in the dye absorbance tail “closes the gap” with the efficiency of the LED as the effective dye concentration is raised by increased loading/dye level.

The most unusual features of the reaction pathway are the absence of a significant amount of chlorocatechol, which would be expected as the primary product of $\text{OH}\cdot$ attack, and the build-up of 1,2,4-benzenetriol and dihydroxymaleic acid. These were identified as the main products of ozonolysis of 4-CP.³³ The exact pathway here remains unclear, but based on the product identification and $\text{OH}\cdot$ scavenging, it can be argued that the reaction is OH radical initiated. Dihydroxymaleic acid suggests the ring opening may occur from the degradation of hydroxy-catechol by an ROS attack at positions with orthohydroxy groups. The reaction mechanism may also involve the attack of $\cdot\text{O}_2-$ on the benzene ring with loss of chlorine from chlorophenol in accordance with several studies.^{36–38,5}

Conclusion

Overall, these results underline the power of the choice of an LED well-matched to the spectrum of the target chro-

mophore. In addition to giving the photochemist another nearly monochromatic light source of satisfactory intensity, simple LED reactors offer the several advantages characteristic of LED operation. The test case further illustrates the potential to exploit dye sensitized TiO₂ photocatalysts for treatment of contaminants. That the pathways implicate ROS other than hydroxyl radical (or equivalent) may suggest differences from TiO₂ alone that can be useful in some cases and a disadvantage in others.

Acknowledgment. We thank Science and Engineering Research Canada (NSERC) for financial support. Part of this work also benefitted from funding from Trans Canada. We thank the staff of the Chemistry Department Instrumentation Facility and Dr. Todd Sutherland for assistance with a number of measurements.

References and Notes

- (1) Mills, A.; Hunte, S. L. *J. Photochem. Photobiol. A: Chem.* **1997**, *108*, 1.
- (2) Hilal, H. S.; Majjad, L. Z.; Zaatar, N.; El-Hamouz, A. *Solid State Sci.* **2007**, *9*, 9.
- (3) Moon, J. Y.; Chung, C. Y.; Kang, M. S.; Yi, J. *Catal. Today* **2003**, *87*, 77.
- (4) Chatterjee, D.; Dasgupta, S.; Rao, N. N. *Sol. Energy Mater. Sol. Cells* **2006**, *90*, 1013.
- (5) Vinodgopal, K.; Stafford, U.; Gray, K. A.; Kamat, P. V. *J. Phys. Chem.* **1994**, *98*, 6797.
- (6) Vinodgopal, K.; Bedja, I.; Kamat, P. V. *Chem. Mater.* **1996**, *8*, 2180.
- (7) Matsunaga, K.; Imanaka, M.; Kenmotsu, K.; Oda, J.; Hino, S.; Kadota, M.; Fujiwara, H.; Mori, T. *Bull. Environ. Contam. Toxicol.* **1991**, *46*, 292.
- (8) Sugimoto, H.; Matsumoto, S.; Sawyer, D. T. *Environ. Sci. Technol.* **1988**, *22*, 1182.
- (9) Iliev, V. *J. Photochem. Photobiol. A: Chem.* **2002**, *151*, 197.
- (10) Mills, A.; Belghazi, A.; Davies, R. H.; Worsley, D.; Morris, S. *J. Photochem. Photobiol. A: Chem.* **1994**, *79*, 131.
- (11) Anderson, C.; Bard, J. A. *J. Phys. Chem.* **1995**, *99*, 9882.
- (12) Zhang, F.; Zhao, J.; Shen, T.; Hidaka, H.; Pelizzetti, E.; Serpone, N. *Appl. Catal., B* **1998**, *15*, 147.
- (13) Lobedank, J.; Bellmann, E.; Bendig, J. *J. Photochem. Photobiol. A: Chem.* **1997**, *108*, 89.
- (14) Cho, Y.; Choi, W.; Lee, C. H. *Environ. Sci. Technol.* **2001**, *35*, 966.
- (15) Wang, W.-Y.; Ku, Y. *Water. Res.* **2006**, *40*, 2249.
- (16) Shie, Je.-L.; Lee, C.-H.; Chiou, C.-S.; Changa, C.-T.; Chang, C.-C.; Chang, C.-Y. *J. Hazard. Mater.* **2008**, *155*, 164.
- (17) Chen, H.-W.; Ku, Y.; Irawan, A. *Chemosphere.* **2007**, *79*, 184.
- (18) Murakoshi, K.; Yanagida, S.; Capel, M.; Castner, E. W. *Interfacial electron transfer dynamics of photosensitized zinc-oxide nanoclusters*; Moskovits, M., Ed.; American Chemical Society: Washington DC, 1997; p 221.
- (19) Rehm, J. M.; McLendon, G. L.; Nagasawa, Y.; Yoshihara, K.; Gratzel, M.; Moser, J. *J. Phys. Chem.* **1996**, *100*, 9577.
- (20) Jones, G. II.; Griffin, S. F.; Choi, C. Y.; Bergmark, W. R. *J. Org. Chem.* **1984**, *49*, 2705.
- (21) Ramakrishna, G.; Ghosh, H. N. *J. Phys. Chem.* **2002**, *106*, 2545.
- (22) Hara, K.; Sayama, K.; Ohga, Y.; Shinpo, A.; Suga, S.; Arakawa, H. *Chem. Commun.* **2001**, 569.
- (23) Mills, A.; Morris, S.; Davies, R. *J. Photochem. Photobiol. A: Chem.* **1993**, *70*, 183.
- (24) Mills, A.; Sawunyama, P. *J. Photochem. Photobiol. A: Chem.* **1993**, *84*, 305.
- (25) Stafford, U.; Gray, K. A.; and Kamat, P. V. *Heterog. Chem. Rev.* **1996**, *3*, 77.
- (26) Stafford, U.; Gray, K. A.; Kamat, P. V. *J. Catal.* **1997**, *167*, 25.
- (27) Cunningham, J.; Sedl'ak, P. *J. Photochem. Photobiol. A: Chem.* **1994**, *77*, 255.
- (28) Parker, C. A. *Proc. R. Soc. London, Ser. A* **1953**, *235*, 518.
- (29) Janzen, E. G.; Blackburn, B. J. *J. Am. Chem. Soc.* **1968**, *90*, 5909.
- (30) Jaeger, C. D.; Bard, A. J. *J. Phys. Chem.* **1979**, *83*, 3146.
- (31) Grela, M. A.; Coronel, M. E. J.; Colussi, A. J. *J. Phys. Chem.* **1996**, *100*, 16940.
- (32) Langford, C. H.; Carey, J. H. *Can. J. Chem.* **1975**, *53*, 2430.
- (33) Epe, B. *Chem.-Biol. Interact.* **1991**, *80*, 239.
- (34) Chen, J.; Eberlein, L.; Langford, C. H. *J. Photochem. Photobiol. A: Chem.* **2002**, *148*, 183.
- (35) Sung, M.; Huang, C. P. *J. Hazard Mater.* **2007**, *141*, 140.
- (36) Li, X.; Cabbage, J. W.; Jenks, S. W. *J. Photochem. Photobiol. A: Chem.* **2001**, *143*, 69.
- (37) Li, X.; Cabbage, J. W.; Tetzlaff, T. A.; Jenks, S. W. *J. Org. Chem.* **1999**, *64*, 8509.
- (38) Sattari, D.; Hill, C. L. *J. Am. Chem. Soc.* **1993**, *115*, 4649.
- (39) Web-link: <http://www.luzchem.com/handbook/LESVis011.pdf>, accessed Dec 04, 2007.

JP804356W